Detecting Brown Adipose Tissue Activity with BOLD MRI in Mice

Arjun Khanna and **Rosa T. Branca**
Chemistry Department, French Family Science Center, Duke University, Durham, NC 27708, USA

Abstract

The recent discovery of active brown adipose tissue (BAT) in adult humans and the correlation found between the activity of this tissue and resting metabolic rate strongly suggest that this tissue may be implicated in the development of obesity in humans, as it is in rodents. Despite the possible physiological role of this tissue in the onset of human obesity, few non-invasive imaging techniques to detect BAT activity in humans exist. The scope of this work is to investigate the possibility of detecting BAT activity using BOLD MRI. Our results show that the strong increase in oxygen consumption and consequent increase in blood deoxyhemoglobin levels following BAT activation lead to a well-localized signal drop in BAT. This strongly suggests the possibility to use BOLD MRI for the non invasive detection of BAT activity.

Introduction

Thermogenesis-induced energy consumption by Brown Adipose Tissue (BAT) is a major component of metabolic balance in mammals. The oxidation of fatty acids and glucose in BAT to generate heat, known as non-shivering thermogenesis (NST), can account for nearly 50% of total energy metabolism in smaller mammals and an even larger fraction in cold-acclimated animals (1). Consistent with these findings, reduced BAT activity has been associated with predisposition to obesity (2,3) and abnormal glucose homeostasis (4) in rodents.

Until recently, active BAT was assumed to be absent in adult humans (5). However, combined ^{18}F-FDG PET/CT scans revealed islets of functionally active BAT in adult humans, with the amount of BAT inversely correlated to body-mass index, suggesting that BAT may play a role in adult human metabolism (6). It has separately been hypothesized that growth of BAT may prevent or correct the development of obesity and associated disorders (1). Because the activity of BAT correlates with predisposition to metabolic disease, visualization of the physiological distribution and activity of BAT are of key interest. Although methods, also from this author, have been developed to detect BAT mass with MRI(7,8), to date the only viable option for functional BAT imaging is CT-guided [18]FDG-PET(9). However,[18]FDG-PET is not specific for BAT activity; the preferred substrates for BAT activity are fatty acids, not glucose. Moreover, because[18]FDG-PET detects glucose uptake by tissues, which is modulated by a variety of external variables, including environmental temperature, anesthesia, glucose levels, and diet, it is likely that[18]FDG-PET underestimates the amount of BAT in adult humans(10,11).Additionally, because [18]FDG-PET delivers harmful ionizing radiation, it is not a viable option for studying BAT activity in healthy and young subjects.

Blood-oxygen-level-dependent (BOLD)MR contrast has been used for the last 20 years in functional studies of the brain(12). Localized increases in cerebral oxygen consumption and blood flow that occur in response to focused neural activation produce a detectable change in the intensity of the MR signal, which can then be used to quantify these physiological parameters (13). BOLD contrast is used not only to detect changes cerebral activity, but also to study oxygenation of kidneys (14), liver (15), and tumors (16), and in general can be used for any tissue in which relative levels of oxy- and deoxy-hemoglobin change in response to a controllable stimulus.

Because BAT is highly vascularized, and because BAT activity results in an increase in oxygen consumption and blood flow to the tissue (17), we hypothesized that BOLD MRI may be used to detect BAT activity. The increase in blood flow is specific to BAT (18)and has been detected in rodents using gadolinium-enhanced MRI (19).However, because the increase in blood flow is accompanied by a nearly 10-fold increase in the rate of BAT oxygen consumption (20), such that the oxygen content of venous blood from active BAT falls below resting levels, we expect to detect a strong MR signal reduction in BAT during metabolic activity.

Methods

All animal studies were conducted with approval of the Duke University Institutional Animal Care and Use Committee. All animals were housed at a constant temperature (20–24°C) in 12-h light/dark cycles and fed standard mouse chow *ad libitum*.

Temperature Studies

For all studies, BAT was pharmacologically stimulated by an intraperitoneal (IP) injection of norepinephrine (NE, norepinephrine bitartrate monohydrate, Sigma-Aldrich, St. Louis, Missouri, USA).To examine the onset and duration of BAT activity by NE, interscapular BAT (iBAT) and rectal temperatures were monitored during NE administration. For these experiments, 3 BALB/C (Charles River, 6–12 wks) female mice were anesthetized with 60–70 mg/kg sodium pentobarbital (Nembutal)via IP injection with maintenance doses of 25 mg/kg delivered every 45 minutes or as needed. A fiber-optic temperature probe was surgically inserted below the pad of iBAT through an interscapular incision and sutured into place. Another probe was inserted 1 cm into the rectum, and another monitored room temperature. To stimulate BAT activity, 2.5 mg/kg of NE in 2 mM ascorbic acid was given IP, and temperatures were monitored continuously before, during and after injection for about 200 minutes.

Imaging Studies

10 BALB/C (Charles River, 6–12 wks) female mice were induced with pentobarbital (60–70 mg/kg) via IP injection. The animals were intubated and mechanically ventilated at 60 breaths/min with a tidal volume of 0.3–0.4 mL at 21% O_2. Two catheters were inserted into the IP cavity and used to administer maintenance doses of pentobarbital (25 mg/kg every 45 min or as needed) and NE (2.5 mg/kg) to elicit BAT activity. The animals were placed supine inside a birdcage ^{1}H coil with 35 mm inner diameter. Rectal and bore temperatures were continuously monitored using MR-compatible temperature probes, and bore temperature was adjusted by air heater to maintain mouse rectal temperature above 28°C. At the end of the study, animals were euthanized by an overdose of pentobarbital.

Four female Caveolin-1 (*Cav1*) mutated mice (Jackson Labs, 6–12 wks) were also used. *Cav1*-null mice exhibit desensitized adrenergic responsiveness, and their BAT activity has been debated. It has been shown, however, that BAT in these mice can be stimulated with

high doses of NE (21). To determine whether BOLD MRI could be used to detect BAT activity in these animals, the animals were prepared as described above, except 4 mg/kg NE was used instead of 2.5 mg/kg to account for decreased adrenergic sensitivity in the mice.

Imaging Parameters

All MRI experiments were performed on a Bruker Biospect Tomograph System (Bruker, Karlsruhe, Germany) equipped with a 7 Tesla horizontal Magnex Scientific magnet(Oxford, UK)with a 21 cm bore and a gradient insert of 42 Gauss/cm maximum intensity. Respiratory-gated gradient echo sequences were first used to locate a 1 cm slice across the iBAT region. T2-weighted axial spin echo sequences were then used to obtain serial images of iBAT every 10–15 minutes before, during, and after NE injection, with TR/TE = 1s/ 14ms, and with a spatial resolution of 117 μm × 234 μm/pixel and a 1 mm slice thickness. Images were then averaged (NEX=4) and respiration-gated to minimize motion-related artifacts.

To examine how T2*-weighting could affect BAT signal, images with T2* weighting of about 2 ms were acquired with an asymmetric spin echo sequence. Briefly, the delay between the excitation and the refocusing pulse was increased by 2 ms (TE/2 =9 ms), while the delay between the refocusing pulse and the center of the acquisition window was kept at 7 ms. This resulted in a mismatch between the center of the echo and the center of k-space of about 2 ms, creating a small (2 ms) T2* star weighting of the images, which was impossible to achieve with our gradient echo sequence.

Image analysis

Signal changes in various tissues following NE stimulation were evaluated using ImageJ 1.38X software (National Institutes of Health, USA). ROIs were placed in the iBAT region, subcutaneous white adipose tissue, skeletal muscle, and Sulzer's vein and its surrounding tissue (Figure 2.c). In each image, the mean signal of each ROI was normalized to the mean signal of pre-contrast images.

A cross-correlation map(Figure 2.e) was obtained using Matlab 2008b (Mathworks, Natick, MA).A 3D data set was constructed using the time series of T2-weighted images acquired before, during, and after stimulation of BAT. For each pixel, we extracted a correlation coefficient between the signal intensity time course and the expected reference function for BAT activity (Figure 2.d) to determine which pixels exhibited a pattern of signal change that correlated with NE stimuli.

Results

Figure 1 illustrates changes in iBAT temperature and rectal temperature induced by IP injection of 2.5 mg/kg NE in a single BALB/C female mouse. Before injection, iBAT and rectal temperatures rapidly decline toward room temperature. Following the injection of NE, iBAT and rectal temperatures increase. Over approximately 40–50 minutes, rectal temperature increases by 4.7°C and BAT temperature increases by 5.5°C. About 60 minutes after the injection of NE, both temperatures start declining, reaching pre-injection levels after about 140 minutes.

In Figure 2, we report changes in mean signal from ROIs drawn around muscle, white adipose tissue, iBAT, and Sulzer's vein with surrounding tissue, along with simultaneous measurements of rectal temperature (Figure 2.a), before, during, and after BAT stimulation induced by a series of two NE injections of 2.5 mg/kg. As expected, rectal temperature reverses its decline and increases by about 1°C following both injections of NE. Concurrently, after each NE injection, iBAT signal intensity falls about 20% and returns to

approximately pre-stimulation levels about 120 minutes after activation. A correlation map between iBAT activity and pattern of signal intensity shows a very strong correlation with the expected stimulation pattern (Figure 2.d) in the iBAT areabut not in surrounding tissues (Figure 2.e). The mean signals of white adipose tissue and muscle are not correlated to NE injection and do not change by more than 10% during the entire experiment. Similar results are obtained in *Cav1*-mutated mice following a single dose of 4 mg/kg NE (Figure 3).

Figure 4 shows serial T2- and T2*-weighted axial images of iBAT in a BALB/C mouse acquired before, during, and after activation by 2.5 mg/kg NE. In T2-weighted images, the iBAT signal falls almost 20% following injection while muscle and white adipose tissue signals do not vary more than 10% and do not exhibit a consistent signal pattern. Greater contrast between active iBAT and surrounding tissues is achieved in T2*-weighted images, in which iBAT signal falls almost 40% following injection while muscle and white adipose tissue signals do not vary by more than 15%.

Discussion and Conclusions

Our objective with this work was to demonstrate MR detection of BAT activity. BAT activity is characterized by an increase in blood flow and oxygen consumption [1], which should be readily observable in T2- and T2*-weighted MR images. To validate this hypothesis, we performed a series of T2- and T2*-weighted MRI experiments on mice before, during, and after BAT activity.

Under pentobarbital-induced anesthesia, BAT activity is readily elicited by NE injection as shown elsewhere(1) and demonstrated herein Figure 1. The initial drop in rectal and iBAT temperature is due to the ablation of central thermoregulation and hypothermic shivering by pentobarbital anesthesia (22),but this drop is arrested and reversed by the injection of NE. NE induces NST in BAT, which leads to an increase in iBAT temperature followed quickly by an increase in rectal temperature. Activity lasts about 60 minutes, after which both iBAT and rectal temperatures peak and start to decline. Over the span of about 250 minutes, BAT activity can be elicited twice, as demonstrated in Figure 2.a.

The activity of BAT is accompanied by a large MR signal drop in the interscapular region, which corresponds to the anatomical location of interscapular iBAT. This signal drop is strongly correlated with BAT activation by NE, demonstrated by the fact that we observe consistent signal loss in BAT only following NE injections that lasts for about 60–70 minutes before returning to normal values(Figure 2.b). The signal reduction systematically follows the expected BAT stimulation pattern (Figure 2.d) and is not observed in nearby tissues. Pixel-by-pixel analysis reveals excellent correlation between BAT stimulation and iBAT signal loss (Figure 2.e).

BAT signal drop can also be detected in *Cav1*-mutated mice. Because these animals exhibit abnormal BAT morphology, altered BAT mitochondrial structure, and decreased WAT lipolysis, their BAT function has been debated (23). Consistent with recent studies on this strain (21), we find that BAT activity can still be detected in these mice, albeit with a higher dose of NE (4 mg/kg). In these animals, signal from BAT drops about 20% following NE injection, and signal from Sulzer's vein BAT drops almost 60%. Again, signal from white adipose tissue and muscle do not exhibit significant changes that correspond to activation (Figure 3). The larger signal drop in Sulzer's vein in this case was probably due to lower partial volume effect in the ROI of these images.

This signal drop is present across both T2- and T2*-weighted images, although T2*-weighted images show greater sensitivity to BAT activity, as demonstrated in Figure 4. This signal drop is clearly the result of a T2- and T2* shortening, though we were unable to

measure this shortening exactly given the presence of different spin components (some with J-coupling) and the impossibility of using short echo time values (<4 ms) in these measurements.

The signal drop that accompanies BAT activity is well-explained by the large increase in oxygen consumption that occurs in this tissue upon stimulation. Unlike in the brain during fMRI, the increase in oxygen consumption during activity of BAT is not sufficiently compensated by the accompanying increase in blood flow; this leads to complete deoxygenation of the venous blood, an accumulation of paramagnetic deoxyhemoglobin in the region, and a faster decay of the MR signal. Sulzer's vein is the primary blood vessel draining blood from the iBAT deposit, so we expected the effect of blood deoxygenation on signal to be greatest in this vessel and nearby tissue. Accordingly, we find that Sulzer's vein and surrounding tissue generally exhibits the largest signal loss of any area in the iBAT region (Figures 2 and 3). Deoxygenation following activation by NE is unique to BAT, so these signal changes are specific to the tissue.

In all our studies BAT was pharmacologically stimulated with NE. NE is the most important activator of BAT and causes thermogenesis in brown adipocytes primarily through the β3 receptor signaling pathway, which ultimately stimulates thermogenesis via lipolysis (1). Physiological stimuli of NST – such as cold exposure or high fat diet – cause activation of BAT through NE release and these natural stimuli produce an effect comparable to IP NE. The magnitude of the response to endogenous or exogenous NE is, on the other hand, a function of BAT recruitment state and thermal prehistory (24).

This study is the first demonstration that BAT activity can easily be detected in mice with standard MRI methods without the use of a contrast agent. Because the signal drop we observe is directly correlated to blood oxygen depletion, these measurements are more indicative of BAT activity than perfusion studies since they reflect metabolic activity instead of changes in blood flow in the tissue. As mentioned in(19), an increase in blood perfusion following activation can be found not only in BAT but also in nearby muscle tissue, confirming that perfusion is not as specific to BAT activity as oxygen consumption. One study (25) finds that postprandial increase of glucose uptake in BAT stimulated by insulin is not accompanied by an increase in perfusion, suggesting that activation of BAT by insulin cannot be studied using perfusion measurements. Indeed, any method that measures blood perfusion is at best an indirect indicator of BAT activity and is inherently less specific than our direct observation of oxygen depletion in the tissue. Direct identification of metabolic activity of BAT that is enabled by our method is therefore more likely to be useful in human studies. Translation of this method to human studies at clinical field strength should be straightforward, given the strong signal reduction observed in both T2 and T2*-weighted images. In this case, because humans lack the large interscapular BAT depots characteristic of rodents, the ability to detect BAT activity with BOLD MRI will strongly depend on the amount and recruitment state of BAT that, as in rodents, seems to be directly correlated to the average metabolic status of BAT. If this is the case, MRI could be a viable alternative to [18]FDG-PET for the study of BAT metabolism in humans. A variety of activators of human BAT have been demonstrated using PET, including NE infusion (26,27), insulin (25), and acute cold exposure (25,28). Rodent studies also suggest that thermogenesis in BAT can be elicited by ephedrine and can be potentiated by dietary methylxanthines such as caffeine (29). These activators may be used to elicit BAT activity in humans. The noninvasive nature of MRI scans may allow longitudinal study in healthy and young subjects that can help unveil the role that BAT plays in the development of human metabolic disorders, including obesity.

In conclusion, we demonstrate the detection of BAT metabolic activity in mice using BOLD MRI experiments. The changes in blood oxygenation that occur in BAT during activity are large enough to be detected using both T2- and T2*-weighted sequences. These changes are specific to BAT, are not present in other tissues, and, most importantly, follow the expected metabolic pattern elicited by NE that has been previously observed in mice. Moreover, if we couple BOLD measurements of net oxygen depletion with MR perfusion measurements like arterial spin labeling, which unlike gadolinium-enhanced perfusion studies is more likely to avoid a "masking" of the BOLD effect, we may be able to extract oxygen consumption rates of BAT during activity.

Acknowledgments

References

1. Cannon B, Nedergaard J. Brown Adipose Tissue: Function and Physiological Significance. Physiological Reviews. 2004; 84(1):277–359. [PubMed: 14715917]

2. Himms-Hagen J, Desautels M. A mitochondrial defect in brown adipose tissue of the obese (ob/ob) mouse: Reduced binding of purine nucleotides and a failure to respond to cold by an increase in binding. Biochemical and Biophysical Research Communications. 1978; 83(2):628–634. [PubMed: 212061]

3. Trayhurn P, Thurlby PL, James WPT. Thermogenic defect in pre-obese ob/ob mice. Nature. 1977; 266(5597):60–62. [PubMed: 840297]

4. Hamann A, Benecke H, Le Marchand-Brustel Y, Susulic VS, Lowell BB, Flier JS. Characterization of insulin resistance and NIDDM in transgenic mice with reduced brown fat. Diabetes. 1995; 44(11):1266–1273. [PubMed: 7589822]

5. Cunningham S, Leslie P, Hopwood D, Illingworth P, Jung RT, Nicholls DG, Peden N, Rafael J, Rial E. The characterization and energetic potential of brown adipose tissue in man. Clin Sci. 1985; 69(3):343–348. [PubMed: 2998687]

6. Cypess AM, Lehman S, Williams G, Tal I, Rodman D, Goldfine AB, Kuo FC, Palmer EL, Tseng Y-H, Doria A, Kolodny GM, Kahn CR. Identification and Importance of Brown Adipose Tissue in Adult Humans. New England Journal of Medicine. 2009; 360(15):1509–1517. [PubMed: 19357406]

7. Branca RT, Warren WS. In vivo brown adipose tissue detection and characterization using water�lipid intermolecular zero-quantum coherences. Magnetic Resonance in Medicine. 2011; 65(2):313–319. [PubMed: 20939093]

8. Hu HH, Smith DL, Nayak KS, Goran MI, Nagy TR. Identification of brown adipose tissue in mice with fat�water IDEAL-MRI. Journal of Magnetic Resonance Imaging. 2010; 31(5):1195–1202. [PubMed: 20432356]

9. Virtanen KA, Nuutila P. Functional imaging of brown adipose tissue. Heart and Metabolism. 2010; 48:15–17.

10. Lee P, Greenfield JR, Ho KKY, Fulham MJ. A critical appraisal of the prevalence and metabolic significance of brown adipose tissue in adult humans. American Journal of Physiology-Endocrinology And Metabolism. 2010; 299(4):E601–E606. [PubMed: 20606075]

11. Lee P, Zhao JT, Swarbrick MM, Gracie G, Bova R, Greenfield JR, Freund J, Ho KKY. High Prevalence of Brown Adipose Tissue in Adult Humans. Journal of Clinical Endocrinology & Metabolism. 2011; 96(8):2450–2455. [PubMed: 21613352]

12. Bandettini PA, Wong EC, Hinks RS, Tikofsky RS, Hyde JS. Time course EPI of human brain function during task activation. Magnetic Resonance in Medicine. 1992; 25(2):390–397. [PubMed: 1614324]

13. van Zijl PCM, Eleff SM, Ulatowski JA, Oja JME, Ulug AM, Traystman RJ, Kauppinen RA. Quantitative assessment of blood flow, blood volume and blood oxygenation effects in functional magnetic resonance imaging. Nat Med. 1998; 4(2):159–167. [PubMed: 9461188]

14. Prasad PV, Edelman RR, Epstein FH. Noninvasive Evaluation of Intrarenal Oxygenation With BOLD MRI. Circulation. 1996; 94(12):3271–3275. [PubMed: 8989140]

15. Haque M, Koktzoglou I, Li W, Carbray J, Prasad P. Functional MRI of liver using BOLD MRI: Effect of glucose. Journal of Magnetic Resonance Imaging. 2010; 32(4):988–991. [PubMed: 20882631]

16. Taylor NJ, Baddeley H, Goodchild KA, Powell MEB, Thoumine M, Culver LA, Stirling JJ, Saunders MI, Hoskin PJ, Phillips H, Padhani AR, Griffiths JR. BOLD MRI of human tumor oxygenation during carbogen breathing. Journal of Magnetic Resonance Imaging. 2001; 14(2): 156–163. [PubMed: 11477674]

17. Foster DO, Frydman ML. Tissue distribution of cold-induced thermogenesis in conscious warm- or cold-acclimated rats reevaluated from changes in tissue blood flow: The dominant role of brown adipose tissue in the replacement of shivering by nonshivering thermogenesis. Canadian Journal of Physiology and Pharmacology. 1978; 57:110–122. [PubMed: 638848]

18. Heim T, Hull D. The blood flow and oxygen consumption of brown adipose tissue in the new-born rabbit. The Journal of Physiology. 1966; 186(1):42–55. [PubMed: 5914257]

19. Sbarbati A, Cavallini I, Marzola P, Nicolato E, Osculati F. Contrast-enhanced MRI of brown adipose tissue after pharmacological stimulation. Magnetic Resonance in Medicine. 2006; 55(4): 715–718. [PubMed: 16506160]

20. Matthias A, Ohlson KBE, Fredriksson JM, Jacobsson A, Nedergaard J, Cannon B. Thermogenic Responses in Brown Fat Cells Are Fully UCP1-dependent. Journal of Biological Chemistry. 2000; 275(33):25073–25081. [PubMed: 10825155]

21. Mattsson CL, Csikasz RI, Shabalina IG, Nedergaard J, Cannon B. Caveolin-1-ablated mice survive in cold by nonshivering thermogenesis despite desensitized adrenergic responsiveness. American Journal of Physiology - Endocrinology And Metabolism. 2010; 299(3):E374–E383. [PubMed: 20530737]

22. Broman, KÄLlskog, Kopp, Wolgast, Broman M. Influence of the sympathetic nervous system on renal function during hypothermia. Acta Physiologica Scandinavica. 1998; 163(3):241–249. [PubMed: 9715736]

23. Cohen AW, Schubert W, Brasaemle DL, Scherer PE, Lisanti MP. Caveolin-1 Expression Is Essential for Proper Nonshivering Thermogenesis in Brown Adipose Tissue. Diabetes. 2005; 54(3):679–686. [PubMed: 15734843]

24. Cannon B, Nedergaard J. Nonshivering thermogenesis and its adequate measurement in metabolic studies. Journal of Experimental Biology. 2011; 214(2):242–253. [PubMed: 21177944]

25. Orava J, Nuutila P, Lidell ME, Oikonen V, Noponen T, Viljanen T, Scheinin M, Taittonen M, Niemi T, Enerback S, Virtanen KA. Different Metabolic Responses of Human Brown Adipose Tissue to Activation by Cold and Insulin. Cell metabolism. 2011; 14(2):272–279. [PubMed: 21803297]

26. Joy RJT. Responses of cold-acclimatized men to infused norepinephrine. Journal of Applied Physiology. 1963; 18(6):1209–1212. [PubMed: 14080744]

27. Kang BS, Han DS, Paik KS, Park YS, Kim JK, Kim CS, Rennie DW, Hong SK. Calorgigenic action of norepinephrine in the Korean women divers. Journal of Applied Physiology. 1970; 29(1): 6–9. [PubMed: 5425039]

28. van Marken Lichtenbelt WD, Vanhommerig JW, Smulders NM, Drossaerts JMAFL, Kemerink GJ, Bouvy ND, Schrauwen P, Teule GJJ. Cold-Activated Brown Adipose Tissue in Healthy Men. New England Journal of Medicine. 2009; 360(15):1500–1508. [PubMed: 19357405]

29. Dulloo AG, Seydoux J, Girardier L. Potentiation of the thermogenic antiobesity effects of ephedrine by dietary methylxanthines: Adenosine antagonism or phosphodiesterase inhibition? Metabolism. 1992; 41(11):1233–1241. [PubMed: 1435297]
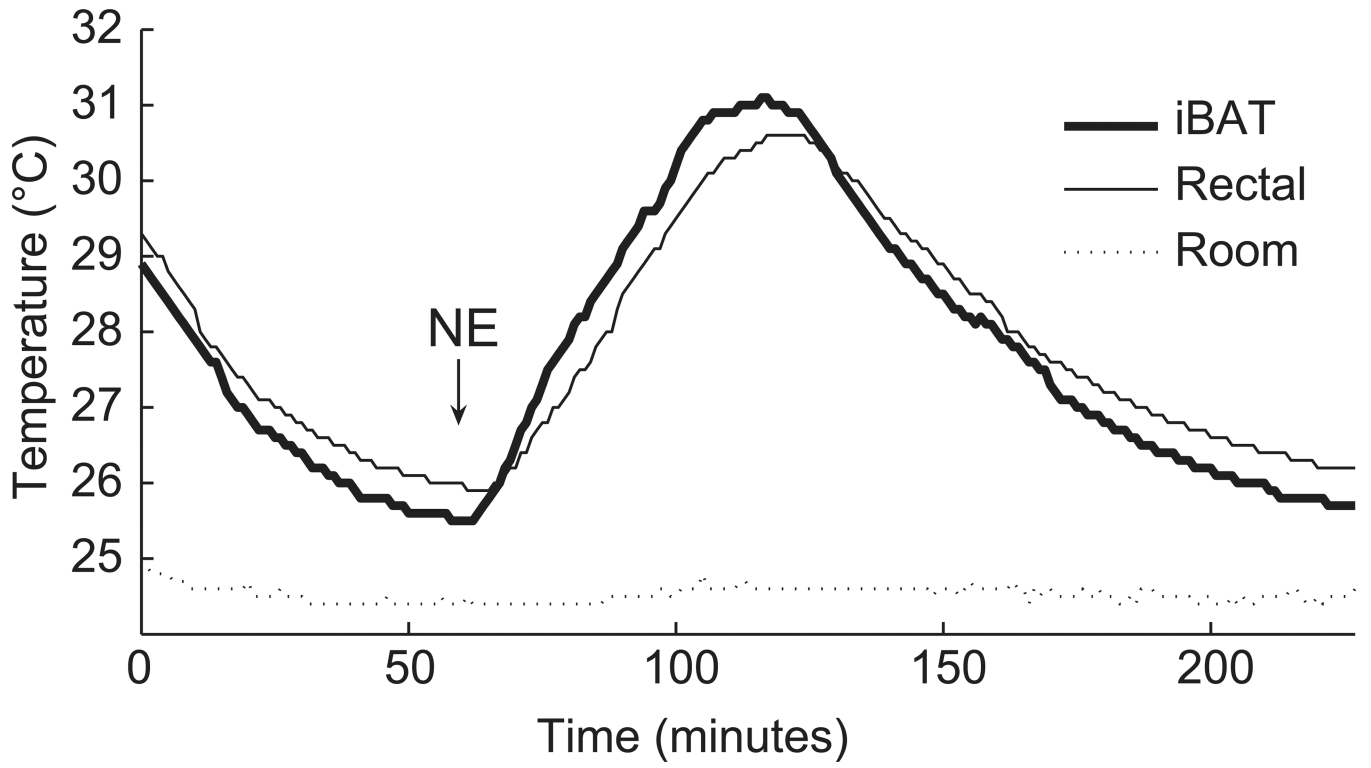
Figure 1.
Interscapular BAT, rectal, and room temperature before, during and after BAT stimulation
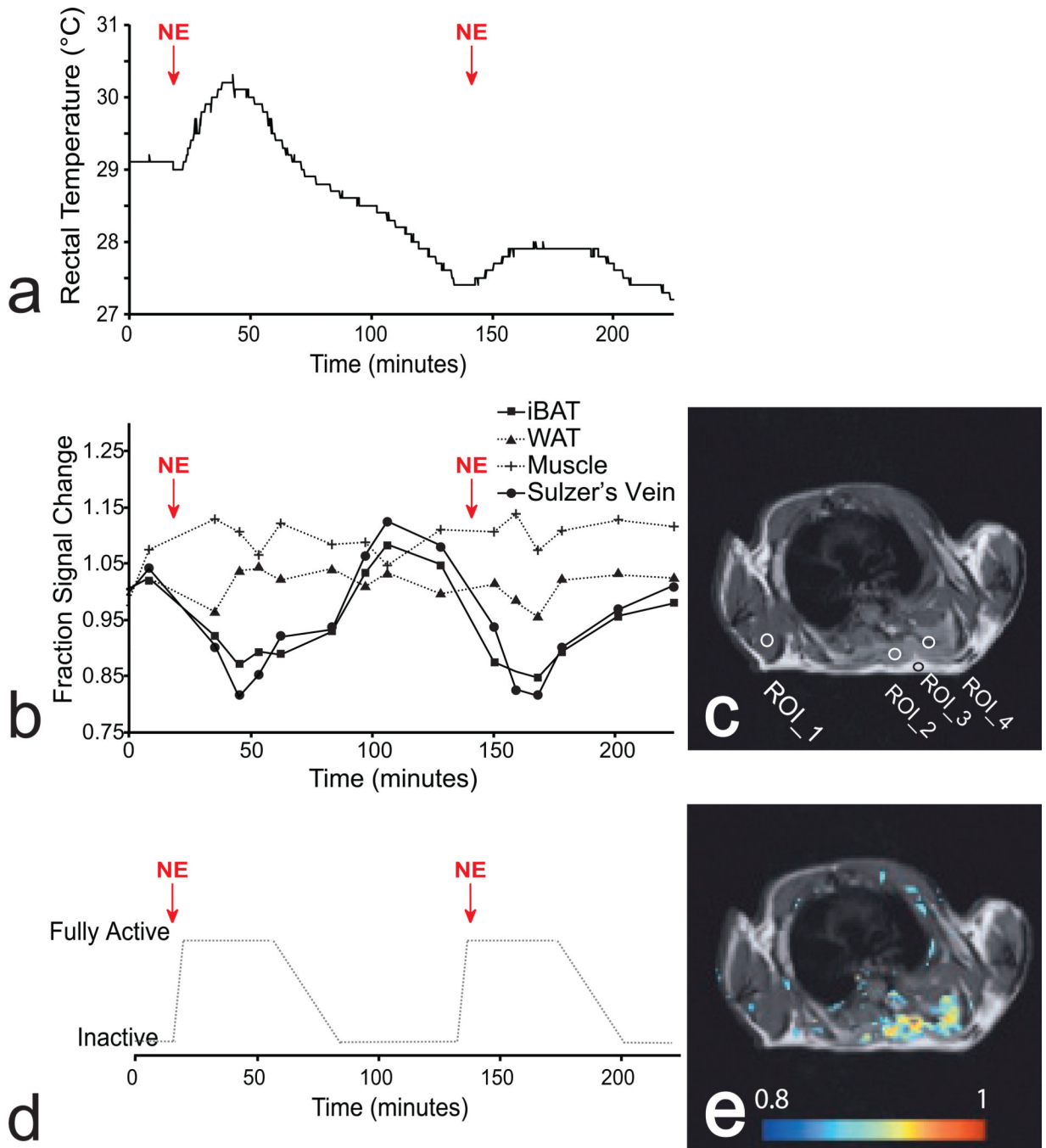by NE injection in a single BALB/C mouse.

Figure 2.
(a) Rectal temperature measured during a single imaging session in a BALB/C mouse before and after a series of two NE injections (2.5 mg/kg each).(b) Signal from iBAT, white adipose tissue (WAT),muscle, and Sulzer's vein and surrounding tissue pre-, during, and after this series of two NE injections. (c) Spin-echo image acquired before the injection of NE showing selected ROIs: muscle (ROI_1), iBAT (ROI_2), WAT (ROI_3), and Sulzer's vein and surrounding tissue (ROI_4).In T2-weighted images, as expected, iBAT appears, when inactive, as a tissue whose intensity is higher than muscle and lower than WAT.(d) Expected BAT activity pattern based on the effect of NE on rectal temperature over two injections in Figure 2.a. After an i.p. injection of NE, BAT soon becomes (1–2 minutes)

fully stimulated. The stimulation lasts for about 60 minutes to then slowly starts to decrease as NE is degraded in the blood. (e) Map showing correlation between the expected BAT activity and the MR signal intensity.
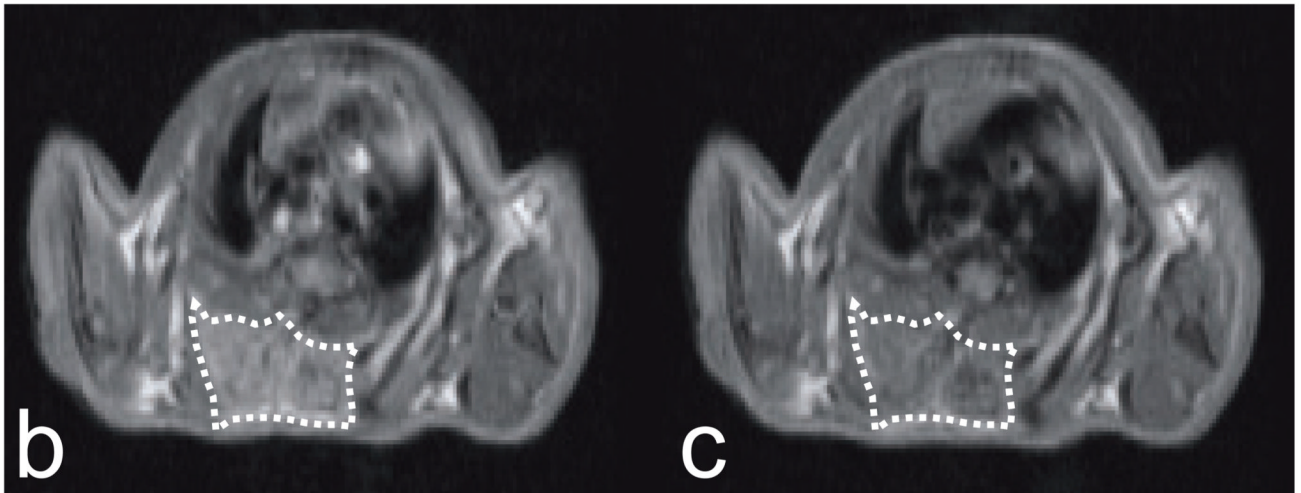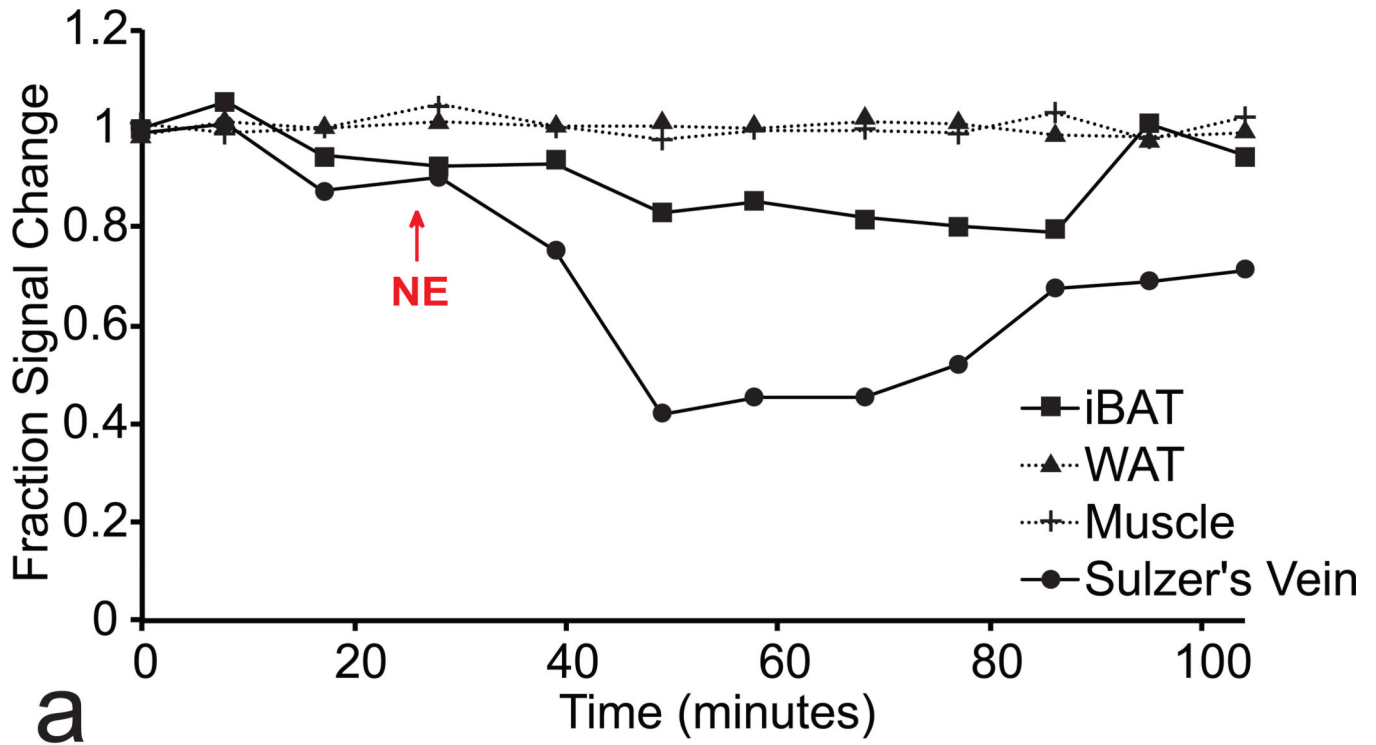
Figure 3.
(a) MR signal behavior of BAT in a *Cav1*-mutated mouse before, during, and after stimulation by NE (4 mg/kg) in various tissues.(b)T2-weighted spin-echo image outlining iBAT (dotted-line) acquired before injection of NE. (c) T2-weighted spin-echo image acquired immediately after injection of NE.
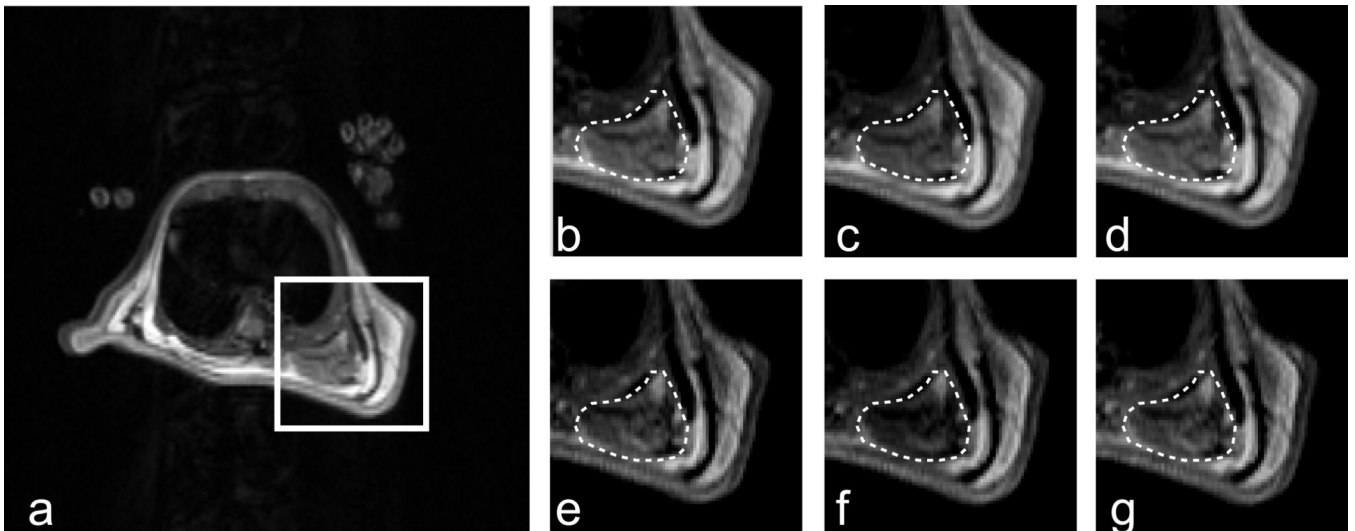
Figure 4.
(a) Axial T2-weighted images acquired before stimulation of BAT highlighting the region containing iBAT (b–d) T2-weighted images outlining iBAT (dotted line) from the indicated region acquired before (b), during (c), and after(d) stimulation of BAT by 2.5 mg/kg NE. (e–g) T2*-weighted images of the same area, acquired with the asymmetric spin-echo sequence, before (e), during(f), and after (g) stimulation of BAT by 2.5 mg/kgNE.